# Resonating group Faddeev approach to deuteron-alpha scattering

K. Hahn and E. W. Schmid
*Institut für Theoretische Physik, Universität Tübingen, D-7400 Tübingen, Federal Republic of Germany*

P. Doleschall
*Central Research Institute for Physics, H-1525 Budapest, Hungary*
(Received 23 July 1984)

The resonating group Faddeev method is formulated and applied to d-$\alpha$ elastic and breakup scattering. The effective interaction of the three-cluster resonating group model for the neutron, proton, and $\alpha$ particle is approximated by the fish bone optical model potential and decomposed into two-body and three-body potentials. The three-body potential is neglected, after being reduced in strength by an off-shell transformation. The two-body potentials are fitted to subsystem on-shell data. Equivalence of subsystem wave functions with resonating group wave functions is checked. Results of the numerical calculation indicate that the three-body observables are sensitive to Pauli effects but are not sensitive to the (unknown) high energy behavior of two-body phase shifts.

## I. INTRODUCTION

The resonating group model[1] has been very successful in describing single-channel and multichannel two-cluster scattering of light nuclei. Without explicit inclusion of cluster distortions and/or compound resonance excitations, this model is simply a folding model with antisymmetrization. The antisymmetrization is important because it prevents a doubling of the nuclear density at short intercluster distances, it reduces the discrepancy of seemingly different cluster descriptions and, therefore, causes the folding prescription to become a good approximation. In a calculation on $\alpha$-$\alpha$ scattering with purely central N-N potential, Tang *et al.*[2] has shown that inclusion of the distortion of the $\alpha$ particles lowers the position of the $l=0$, 2, and 4 rotational resonances by only $\sim 0.3$ MeV. This shift is even smaller than the shift which is produced, for instance, by the uncertainty in the exchange mixture of the phenomenological nucleon-nucleon potential. This finding indicates that tightly bound clusters of nucleons sometimes behave like elementary particles, even in situations where they strongly interpenetrate.

The success of the resonating group model with two-cluster reactions has stimulated the desire to extend the calculations to three-cluster reactions. This, however, has proved to be rather difficult. The complicated dynamics of a three-body system, in connection with the complicated exchange interactions of resonating group theory, has just been too much for practical calculations. Attempts to employ $R$-matrix theory,[3] $K$-harmonics expansion,[4] or wave packet discretization[5] have failed. Recently, Yahiro *et al.*[6] could show by a tremendous numerical effort that a discretization of the breakup channel, similar to the one proposed in Ref. 7, Sec. 8.3.2, converges. In an unpublished report[8] one of us proposed a resonating group Faddeev method. The main idea was to seriously consider a three-cluster resonating group equation to be a three-*particle* Schrödinger equation, to analyze and simplify the effective interaction, and to then use existing Faddeev methods to solve the dynamical problem. The paper has started a series of investigations which has led to the results of the present paper. The intermediate steps include a generalization of resonating group theory to $N$ clusters,[9,10] the two- and three-cluster fish bone optical model,[11,12] the unitary interpolation method,[13] a study of the Pauli barrier effect, and an investigation on the importance of the three-cluster Pauli potential.[14,15] In the present paper, we adapt a Faddeev code[16] to higher rank separable potentials (with positive-energy bound states) and use it to calculate the d-$\alpha$ elastic scattering cross section, the analyzing powers, and the differential cross section of the breakup reaction $\alpha$(d,p$\alpha$)n.

In Sec. II, the numerical method employed to solve the Faddeev equation will be shortly reviewed. The reduction of the six-nucleon problem to an effective three-body problem, of a form suitable for the Faddeev code, will be the topic of Sec. III. Results of the resonating group Faddeev calculation are given in Sec. IV and a summary is given in Sec. V.

## II. NUMERICAL ACCURACY OF THE FADDEEV CALCULATIONS

We are using a computer code which has been tested and used in several three-nucleon calculations.[16] Because of the rather sharp $^2P_{3/2}$ resonance near 1 MeV (c.m.) in the N-$\alpha$ system, the np$\alpha$ system is numerically more tricky than the three-nucleon system. We have tested numerical stability of the elastic and breakup observables by varying both the number of mesh points and the number of partial waves. Stability was reached with the number of mesh points $(N_1,N_2,N_3)=(16,6,7)$ in each one of the coupled equations, and partial waves up to $J^P=9^-$. We repeated, for comparison, calculations of Charnomordic *et al.*[17] and Koike,[18] who used the contour deformation method with rank-1 subsystem potentials. The elastic differential cross sections and analyzing powers agreed well with those calculated by the contour deformation method,

 

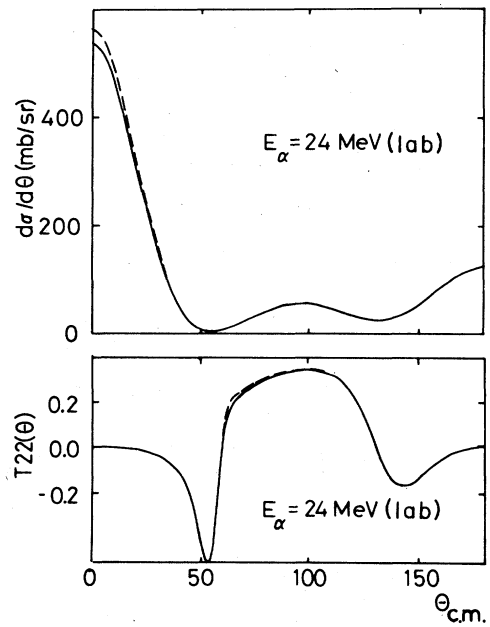


FIG. 1. Elastic differential cross section and tensor analyzing power $T22$, calculated with the present code (solid lines) in comparison with results by Charnomordic *et al.* (broken lines).

see Fig. 1. In the breakup case the agreement of differential cross sections was not as good. In certain kinematical regions, differences of up to 15% of the maximum have been found, see Fig. 2. In the discussion of the resonating group Faddeev method, Sec. IV, we use breakup results only of those kinematical regions where the cross sections of both numerical procedures agreed well with each other in the test examples.

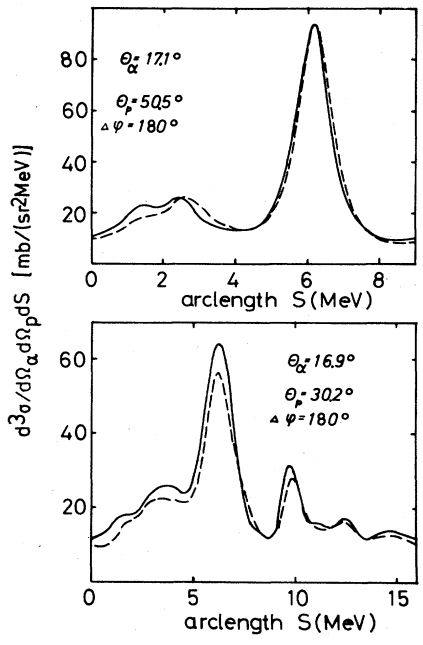


FIG. 2. Breakup cross sections at $E_\alpha = 15$ MeV (lab) calculated with the present code (solid lines) in comparison with results by Koike (broken lines).

## III. REDUCTION OF THE SIX-NUCLEON PROBLEM TO AN EFFECTIVE THREE-BODY PROBLEM

The reduction of the six-nucleon problem to a three-body problem, one of the bodies being an $\alpha$ particle, has been described in Ref. 8. There, the effective interactions including distortion corrections and compound resonance excitations have been defined. An extension of the resonating group model to an arbitrary number of particles and clusters has been given in Refs. 9 and 10. In the general theory, a difficulty arises from the fact that the space of distortion functions is no longer a space of square integrable functions, when there are more than two clusters; in the three-cluster case, this difficulty, however, is not yet serious.[10]

In the present paper we are dealing with the npα system and we want to treat the $\alpha$ particle as an inert particle. This means that we have to restrict the range of energies for which the present approach is applicable. At $E = 12.096$ MeV (c.m.) above the npα threshold the $\alpha$ particle can breakup because this is the threshold of the t-$^3$He channel. We have to stay well below this threshold and we, therefore, limit the range of scattering energies to $-E_d < E < 10$ MeV (c.m.), where $E$ is the energy relative to the npα threshold and $E_d$ is the deuteron binding energy. From the already mentioned results by Tang *et al.*[2] we expect that neglection of the $\alpha$-particle distortion will be a rather good approximation in this energy range. The distortions of the deuteron will, of course, be fully included in the three-body calculation. At the present time, we are not performing a bound state calculation for $^6$Li.

In the following five subsections we discuss the resonating group Faddeev method. A sequence of steps will lead us from the Schrödinger equation for the nucleons via the resonating group model to the three-body Faddeev equation.

### A. The resonating group model and the fish bone optical model

In the no-distortion approximation, the resonating group equation for the npα system reads

$$\langle \Phi\delta\chi \mid \mathcal{A}(H-E)\mathcal{A} \mid \Phi\chi \rangle = 0 \,. \tag{1}$$

The internal motion state $\Phi$ describes the internal properties of the $\alpha$ particle and also contains the spin and isospin of the additional neutron and proton. The relative motion state $\chi$ describes the motion of the neutron, the proton, and the center of mass of the $\alpha$ particle, relative to each other, and $\delta\chi$ is an arbitrary variation of $\chi$. The Hamiltonian $H$ is a six-particle Hamiltonian with a phenomenological N-N interaction, $E$ is the total energy, and $\mathcal{A}$ is the antisymmetrizer.

In the approximation given by Eq. (1) the resonating group model is a simple folding model with antisymmetrization. Nevertheless, the effective potentials which are obtained when Eq. (1) is written as an integro-differential equation for $\chi$ are very complicated. This is one reason why one tries to further simplify the equation. The second reason is that the resonating group equation (1) does not contain any free parameters. In some respect, this is an advantage of the resonating group model. In a

three-cluster calculation, however, it becomes a disadvantage. The effort of doing a three-body calculation and comparing results with experiment is not justified when the two-body observables already disagree with experiment. A three-body observable is sensitive to off-shell properties of the two-body subsystems, but, in order to extract information from this feature, the subsystem potentials must reproduce the two-body observables. This is why the fish bone optical model has been introduced.[11,12]

In the three-cluster fish bone model, the effective interaction of three clusters $a$, $b$, and $c$ following from Eq. (1) is analyzed and split into a dominant part and a residual part [see Ref. 12, Eq. (21a)]. The dominant part rigorously contains the exchange interaction arising from the energy term and from the kinetic energy operator. The exchange interaction arising from potential energy is only contained in a certain approximation. The approximation is such that the nucleon-nucleon interaction enters only after being folded with unexcited cluster states. The further details of the nucleon-nucleon interaction enter into a residual interaction term. If the latter term is dropped and compensated by the introduction of fitting parameters in the above-mentioned folding potential, one arrives at the three-cluster fish bone optical model. The interaction $\overline{\mathscr{V}}_{abc}$ of the three-cluster fish bone optical model contains effective two-cluster interactions $\overline{\mathscr{V}}_{ab}$, $\overline{\mathscr{V}}_{bc}$, and $\overline{\mathscr{V}}_{ca}$, and an effective three-cluster interaction $\overline{V}_P$. The latter is called the three-cluster Pauli potential, because it arises from antisymmetrization. We have [see Ref. 12, Eq. (25)]

$$\overline{\mathscr{V}}_{abc}=\overline{\mathscr{V}}_{ab}1_c+\overline{\mathscr{V}}_{bc}1_a+\overline{\mathscr{V}}_{ca}1_b+\overline{V}_P\ . \tag{2}$$

The potentials $\overline{\mathscr{V}}_{ab}$, $\overline{\mathscr{V}}_{bc}$, and $\overline{\mathscr{V}}_{ca}$ are identical to the potentials of the two-cluster fish bone optical model [see Ref. 11, Eq. (50)],

$$\overline{\mathscr{V}}=V-\sum_{i,j}|u_i\rangle\langle u_i|(T+V-\epsilon)|u_j\rangle\overline{M}_{ij}\langle u_j|\ . \tag{3}$$

In this equation we have omitted the subsystem index ($ab$, $bc$, or $ca$) and the partial wave index; the effective potentials carry a bar because we are using the $\overline{M}$ version of the fish bone optical model. The states $|u_i\rangle$ are eigenstates of the two-cluster norm kernel,

$$\langle\Phi\vec{r}|\mathscr{A}|\Phi u_i\rangle=(1-\eta_i)u_i(\vec{r})\ , \tag{4}$$

where $\Phi$ denotes the product of the cluster ground states and $\vec{r}$ is the center of mass distance of the two clusters. For each partial wave, the eigenvalues $\eta_i$ are ordered in such a way that $|\eta_{i+1}|\le|\eta_i|$ is valid. The matrix $\overline{M}_{ij}$ is then given by

$$\begin{aligned}\overline{M}_{ij}&=1-\frac{1-\eta_i}{[(1-\overline{\eta}_i)(1-\overline{\eta}_j)]^{1/2}},\quad i\le j\\&=1-\frac{1-\eta_j}{[(1-\overline{\eta}_i)(1-\overline{\eta}_j)]^{1/2}},\quad i>j\\\overline{\eta}_i&=0\ \text{ if }\eta_i=1\\&=\eta_i\ \text{ if }\eta_i\neq1\ .\end{aligned} \tag{5}$$

n Eq. (3), $T$ is the kinetic energy operator of the two-cluster relative motion. In the starting approximation, the potential $V$ is the double folding potential of the two-cluster system. It contains fitting parameters to modify its depth and shape, in order to reproduce experimental phase shifts. The parameter $\epsilon$ is used to remove Pauli-forbidden norm kernel eigenstates (redundant states) from the physical part of the relative motion spectrum. They become (positive energy) bound states of the two-cluster equation at energy $\epsilon$. In the present paper, the three clusters $a$, $b$, and $c$ will be n, p, and $\alpha$, respectively; the parameter $\epsilon$ will be $+500$ MeV.

### B. Fit to subsystem phase shifts

For the n-p subsystem we use a separable rank-1 potential in the coupled $^3S_1$-$^3D_1$ partial wave with parameters given in Ref. 16. We neglect the interaction in higher partial waves and, since we also neglect isospin mixing, the $^1S_0$ partial wave will not contribute in the d-$\alpha$ scattering calculation.

For the n-$\alpha$ and p-$\alpha$ subsystems we use a charge independent potential in the form of Eq. (3) in the $^2S_{1/2}$, $^2P_{1/2}$, and $^2P_{3/2}$ partial waves, and neglect the interaction in higher partial waves. For the internal motion state of the $\alpha$ particle we assume a single Gaussian function. In this case, the norm kernel eigenfunctions $u_i$ are harmonic oscillator functions and the norm kernel eigenvalues are known.[19] For the $\alpha$ particle we choose the width parameter $a=0.55$ fm$^{-2}$, which corresponds to an rms radius of 1.4 fm for the bare nucleon distribution and $\sim1.6$ fm for the charge distribution. The norm kernel eigenvalues are 1, $1/16$, $1/16^2,\ldots,$ in the $^2S_{1/2}$ wave and $-1/4$, $-1/(4\cdot16)$, $-1/(4\cdot16)^2,\ldots,$ in the $^2P_{1/2}$ and $^2P_{3/2}$ waves. The first eigenstate of the $^2S_{1/2}$ wave is Pauli forbidden. By choosing $\epsilon=500$ MeV we turn it into a bound state at $+500$ MeV. For the direct part $V$ of the potential $\overline{\mathscr{V}}_{N\alpha}$ we use a local potential of Woods-Saxon shape with a spin-orbit part,

$$\begin{aligned}V(r)=&\frac{-V_w}{\left[1+\exp\left[\dfrac{r-k_1}{k_2}\right]\right]}\\&+[j(j+1)-l(l+1)-s(s+1)]\\&\times\frac{V_{w,\mathrm{so}}}{r}\frac{d}{dr}\frac{1}{\left[1+\exp\left[\dfrac{r-a_1}{a_2}\right]\right]}\ .\end{aligned} \tag{6}$$

The parameters are given in Table I. With these parameters, the fish bone optical model potential approximately reproduces the experimental n-$\alpha$ phase shifts[20] as shown

TABLE I. Parameters of the Woods-Saxon potential, Eq. (6).

| | $^2S_{1/2}$ | $^2P_{1/2}$ | $^2P_{3/2}$ |
|---|---|---|---|
| $V_W$ (MeV) | 34.6474 | 36.8507 | 35.0000 |
| $k_1$ (fm) | 2.3555 | 2.3236 | 2.5206 |
| $k_2$ (fm) | 0.3726 | 0.3238 | 0.2312 |
| $V_{w,\mathrm{so}}$ (MeV) | | 32.9296 | 5.3272 |
| $a_1$ (fm) | | 1.1190 | 1.6717 |
| $a_2$ (fm) | | 0.3137 | 1.1189 |

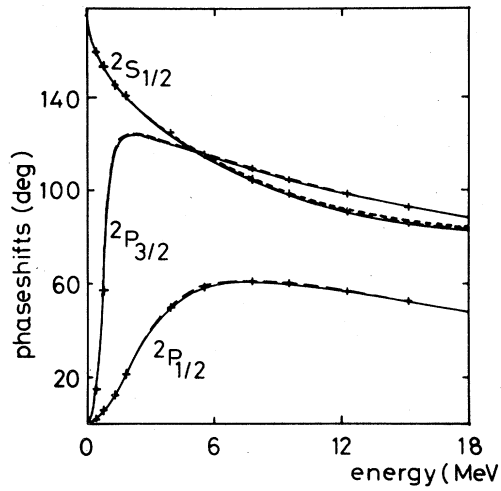


FIG. 3. Neutron-alpha phase shifts of the fish bone optical model (solid lines), of a phenomenological model by Charnomordic *et al.* (broken lines), and of a second phenomenological model (dotted line, only $^2S_{1/2}$ wave). Experimental data by Satchler *et al.* (crosses).

in Fig. 3. Above 18 MeV (c.m.) the phase shift fit becomes ambiguous because of the presence of inelastic channels which, however, are closed in our three-body calculation. We are using this degree of freedom to reproduce the phase shifts of the phenomenological potential of Charnomordic *et al.*[17] up to about 400 MeV. This will enable us to study off-shell effects by comparing Faddeev results of the phenomenological model by these authors with results of the present resonating group Faddeev calculation.

### C. Separable potential approximation

Our Faddeev code uses separable two-body $t$ matrices. It would be possible to generate them directly from the potential of Eq. (3) by a truncated Hilbert-Schmidt expansion. We are getting more physical insight, however, by using an interpolation method which has been described and tested earlier.[13] The method is similar to the one by Ernst, Shakin, and Thaler[21] and differs only by the inclusion of positive energy bound states. The separable potential is generated by the condition that it reproduces the positive energy bound state(s) of the original potential together with the wave functions at a chosen set of interpolation energies. The rank of the separable potential is equal to the number of positive energy bound states plus the number of interpolation energies.

In the present case we use a rank-3 potential in the $^2S_{1/2}$ partial wave and rank-2 potentials in the $^2P_{1/2}$ and $^2P_{3/2}$ waves. The $^2S_{1/2}$ potential has to reproduce the positive energy bound state at 500 MeV. The interpolation energies are chosen to be $E_1=5$ MeV and $E_2=30$ MeV. In the $^2P_{1/2}$ wave the interpolation energies are 10 and 20 MeV and in the $^2P_{3/2}$ wave they are 0.96 and 20

TABLE II. Coupling parameters $\Lambda_{ij}$ of the rank-3(2) separable potentials, Eq. (7).

| | | $\Lambda_{ij}$ coupling constants | | |
|---|---|---|---|---|
| $^2S_{1/2}$ | $j^i$ | 1 | 2 | 3 |
| | 1 | 483.2744 | −0.4650 | −0.0389 |
| | 2 | −0.4650 | −18.2855 | 0.4562 |
| | 3 | −0.0389 | 0.4562 | 9.1932 |
| $^2P_{1/2}$ | $j^i$ | 1 | 2 | |
| | 1 | −18.3947 | −3.3111 | |
| | 2 | −3.3111 | −4.0157 | |
| $^2P_{3/2}$ | $j^i$ | 1 | 2 | |
| | 1 | −30.0542 | −5.0052 | |
| | 2 | −5.0052 | −8.0470 | |

TABLE III. Expansion coefficients of the form factors $\lambda_i$ of the separable potentials, Eq. (8).

| $^2S_{1/2}$ $\alpha_{1k}$ | $^2S_{1/2}$ $\alpha_{2k}$ | $^2S_{1/2}$ $\alpha_{3k}$ | $^2P_{1/2}$ $\alpha_{1k}$ | $^2P_{1/2}$ $\alpha_{2k}$ | $^2P_{3/2}$ $\alpha_{1k}$ | $^2P_{3/2}$ $\alpha_{2k}$ |
|---|---|---|---|---|---|---|
| −0.9996 | 0.0252 | −0.0055 | 0.7901 | −0.3729 | 0.9023 | −0.2688 |
| 0.0289 | 0.8734 | −0.1894 | −0.0513 | 0.6493 | 0.3732 | 0.6874 |
| | 0.4663 | 0.3578 | −0.2728 | −0.0563 | 0.0862 | 0.4880 |
| | 0.0472 | 0.7742 | −0.3682 | −0.2388 | −0.0959 | 0.3844 |
| | −0.0634 | 0.4279 | −0.3012 | −0.3610 | −0.1257 | 0.1488 |
| | −0.0839 | 0.1625 | −0.1852 | −0.3361 | −0.0893 | −0.0210 |
| | −0.0628 | −0.0078 | −0.0759 | −0.2414 | −0.0372 | −0.1065 |
| | −0.0335 | −0.0838 | 0.0054 | −0.1296 | 0.0050 | −0.1238 |
| | −0.0098 | −0.0972 | 0.0554 | −0.0308 | 0.0294 | −0.0991 |
| | 0.0050 | −0.0800 | 0.0793 | 0.0414 | 0.0373 | −0.0578 |
| | 0.0117 | −0.0518 | 0.0844 | 0.0859 | 0.0336 | −0.0169 |
| | 0.0129 | −0.0248 | 0.0780 | 0.1066 | 0.0237 | 0.0145 |
| | 0.0111 | −0.0046 | 0.0658 | 0.1093 | 0.0121 | 0.0333 |
| | 0.0079 | 0.0083 | 0.0515 | 0.1006 | 0.0016 | 0.0401 |
| | 0.0046 | 0.0148 | 0.0377 | 0.0855 | −0.0059 | 0.0379 |
| | 0.0018 | 0.0163 | 0.0257 | 0.0681 | −0.0105 | 0.0299 |
| | −0.0002 | 0.0146 | 0.0161 | 0.0507 | −0.0121 | 0.0195 |
| | −0.0014 | 0.0113 | 0.0088 | 0.0351 | −0.0114 | 0.0087 |
| | −0.0021 | 0.0078 | 0.0033 | 0.0221 | −0.0091 | −0.0006 |
| | −0.0023 | 0.0045 | −0.0006 | 0.0119 | −0.0060 | −0.0077 |

MeV. The obtained potentials have the form

$$\mathcal{V}=\sum_{i,j=1}^{r}|\lambda_i\rangle\Lambda_{ij}\langle\lambda_j| \ . \tag{7}$$

As a representation basis for the form factors we use the norm kernel eigenstates,

$$|\lambda_i\rangle=\sum_k a_{ik}|u_k\rangle \ . \tag{8}$$

The matrix elements $\Lambda_{ij}$ and expansion coefficients $a_{ik}$ are given in Tables II and III. With the chosen rank, the separable potentials reproduce the wave functions of the original potentials of Eq. (3) very well in the energy range 0—40 MeV. We do not show the plots because, with the usual scale of wave function plots, the curves coincide.

It has been stated already that the unitary interpolation method gives us some physical insight. First, we observe that the only subsystem information which will enter into the Faddeev equations is a set of wave functions together with the nonuniqueness feature of resonating group wave functions. [Pauli-Forbidden relative motion states are trivial solutions of Eq. (1) and may be added to the solution $\chi$ at all energies, or, if one takes provisions like we did in Eq. (3), only at a chosen energy $\epsilon$.] This will allow us to look for Pauli effects in terms of wave functions rather than in terms of nonlocal potentials. Second, we can test a feature which is crucial for the resonating group Faddeev method. The effective N-$\alpha$ potential of Eq. (3) defines wave functions also at energies which are much higher than 18 MeV. But we know that these wave functions do not correctly describe N-$\alpha$ scattering because many inelastic channels are open. If the results of our Faddeev calculations were sensitive to the high-energy behavior of the effective N-$\alpha$ potential, the resonating group Faddeev method would be useless. With the unitary interpolation method we can check this sensitivity. In the case of the $^2S_{1/2}$ partial wave we construct a rank-4 separable potential as an alternative to the rank-3 potential. The rank-4 potential has a third interpolation energy $E_3=120$ MeV, which means that it reproduces wave functions of the potential of Eq. (2) up to about 140 MeV. Figure 4 shows the phase shifts of the original potential and of the rank-3 and rank-4 potentials in a wide energy range. The rank-3 and rank-4 potentials differ in the range 40—300 MeV by up to 50 deg of phase shift. We then perform two Faddeev calculations, the first with the rank-3, the second with the rank-4 potential in the $^2S_{1/2}$ partial wave, while all remaining interactions are kept fixed. The comparison of the differential cross sections and of the analyzing powers in elastic d-$\alpha$ scattering and of the differential cross sections in the breakup reaction d($\alpha$,p$\alpha$)n shows that the rank-3 potential produces practically the same results as the rank-4 potential. The analogous investigations in the case of the $^2P_{1/2}$ and $^2P_{3/2}$ partial waves show that, in low energy d-$\alpha$ scattering, the Faddeev results are practically independent of the behavior of the effective N-$\alpha$ potential at energies above 40 MeV.

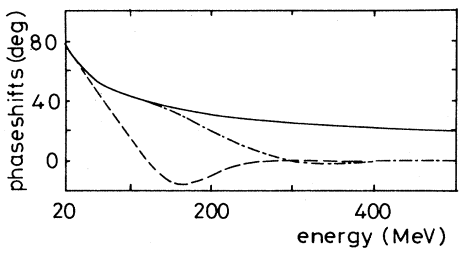


FIG. 4. Comparison of $^2S_{1/2}$ neutron-alpha phase shifts at higher energies; fish bone optical model (solid line), rank-3 separable potential (broken line), and rank-4 separable potential (dashed-dotted line).

### D. Comparison of the separable potential model with the resonating group model

By the fish bone optical model and the unitary interpolation method we have obtained separable potentials which reproduce experimental N-$\alpha$ phase shifts and which approximately contain the Pauli effect by their half off-shell behavior. We want to check now whether there is a substantial difference between the interaction of the resonating group model and our separable potentials.

The resonating group interaction is strongly influenced by the Pauli principle. They are also influenced by the particular choice of a nucleon-nucleon interaction, but this influence is smaller. Since the nucleon-nucleon interaction is not known from first principles, the effective interactions of the resonating group model are uncertain to some extent. If we plot the relative motion wave functions of the resonating group model for a given energy, but for different microscopic interactions, we expect them to lie in a narrow band, provided that the phase shifts are similar. Our hope is that the wave function of the fish bone optical model will also lie in that band. Only if this turns out to be true, then the present method may be called a "resonating group Faddeev method."

Reichstein *et al.* have presented four different resonating group potentials for N-$\alpha$ scattering,[22] which are denoted there by I, II, III, and IV. They are phase equivalent within $\sim$3 deg and differ mainly by a different treatment of the spin-orbit interaction. For our test we have chosen two different shapes for the direct part of the fish bone optical model potential, a Gaussian and a Woods-Saxon shape, and have fitted the parameters to reproduce the phase shift of potential III by Reichstein *et al.* In order to make a comparison of wave functions possible, we have transformed the wave functions obtained from the Reichstein *et al.* potentials by the same off-shell transformation which also leads from the $M$ version to the $\overline{M}$ version of the fish bone optical model and which would make the Reichstein *et al.* potentials energy independent [see Ref. 11, Eq. (45)]. Figure 5 shows the comparison at 10 MeV; at other energies the pictures look similar.

In the $^2S_{1/2}$ partial wave, the resonating group wave functions lie, indeed, in a very narrow band. With a direct potential of Gaussian shape, the wave function of the fish bone optical model lies within this band. With a Woods-Saxon shape, the wave function of the fish bone optical model lies a little outside, but not much. The reason is that the direct parts of the Reichstein *et al.* potentials have a Gaussian shape.

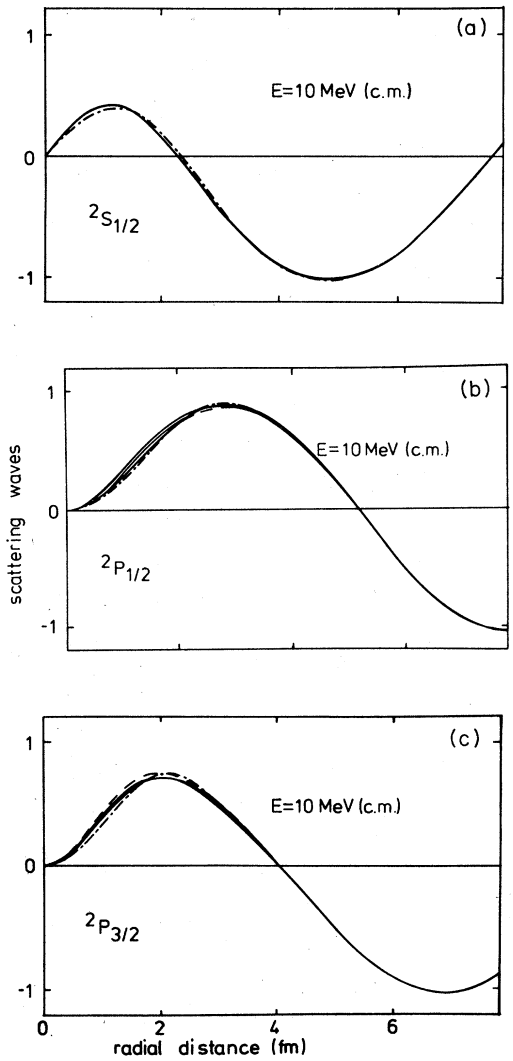


FIG. 5. Comparison of neutron-alpha wave functions. Resonating group models by Reichstein *et al.* (solid lines), and the fish bone optical model with a Gaussian direct potential (broken lines) and with a Woods-Saxon direct potential (dashed-dotted lines).

In the $^2P_{1/2}$ and $^2P_{3/2}$ partial waves the band of resonating group wave functions is wider than in the $^2S_{1/2}$ wave. Again, the wave function of the fish bone optical model with a Gaussian (central) direct part lies, in or close to, that band and the one with a Woods-Saxon shape lies a little outside.

We decided to use the Woods-Saxon shape, in our further calculations, because it seems to be more realistic than the Gaussian shape. The Gaussian shape is correct when the $\alpha$ particle wave function is assumed to be a single Gaussian function and when the nucleon-nucleon potential is of Gaussian shape. When the nucleon-nucleon potential is assumed to have a hard core, or some other strongly repulsive core, the direct part of the effective cluster-cluster potential becomes less attractive at short distances[23] and a Woods-Saxon shape seems to be more appropriate than a Gaussian shape.

### E. Importance of three-body potentials

Effective three-body forces in systems of three fermion clusters have become a rather new and interesting field of research. It is known that they arise by the Pauli potential, by cluster distortions, and by the hard core of the microscopic potential.[8–10,23] A numerical test has shown that the three-body Pauli potential is very strong in the usual resonating group model with an energy-dependent exchange interaction.[15]

A strong three-body potential would be unpleasant in a Faddeev calculation. Therefore, it has been suggested[24] to reduce its strength by an off-shell transformation. It has been found that the three-body Pauli potential is greatly reduced by an off-shell transformation which renormalizes the relative motion states of clusters.[12,15] Renormalization means that the norm of the relative motion state becomes identical to the norm of the corresponding microscopic state, which is not true in the usual resonating group model and in the corresponding $M$ version of the fish bone optical model. The off-shell transformation which achieves the renormalization is the same, in the resonating group model and in the fish bone optical model. In the latter it leads to the $\overline{M}$ version of the model which we are using in the present paper. The off-shell transformation not only reduces the strength of the three-body Pauli potential, it also leads to an energy-independent exchange interaction. It has been found that smallness of the three-body potential, correct normalization of the relative motion wave function, and the probability interpretation of the relative motion wave function are related concepts.[25]

In the present paper, we are neglecting the three-body Pauli potential $\overline{V}_P$ and we are neglecting the three-body potentials which would arise from hard core correlations and from cluster distortions; we are also neglecting distortion effects in the two-body potentials. By these neglections we are making the transition from a six-particle theory to a three-body theory. In the three-body theory, all information about the internal properties of the bodies is represented by the interaction.

Our present assumption that the three-body forces are small is based on rather simple numerical examples.[26,27] We are aware of the need for more investigations on three-body forces.

## IV. FADDEEV RESULTS AND DISCUSSION

Numerical Faddeev calculations were performed for incident alpha-particle energies $E_\alpha = 24$ and 15 MeV (lab). Results for d-$\alpha$ elastic scattering are depicted in Figs. 6 and 7. Some breakup results are shown in Figs. 8 and 9. More results are presented and discussed in Refs. 28 and 29. In all Faddeev calculations the Coulomb potential has been switched off.

In elastic scattering the agreement between theory and experiment[30] is satisfying, with discrepancies mainly at forward angles. Let us discuss the possible reasons for the discrepancies. First, there is the neglection of the Coulomb potential. This should have a large influence at small scattering angles. Also, neglection of the Coulomb interaction shifts the position of the $^5$Li resonances.

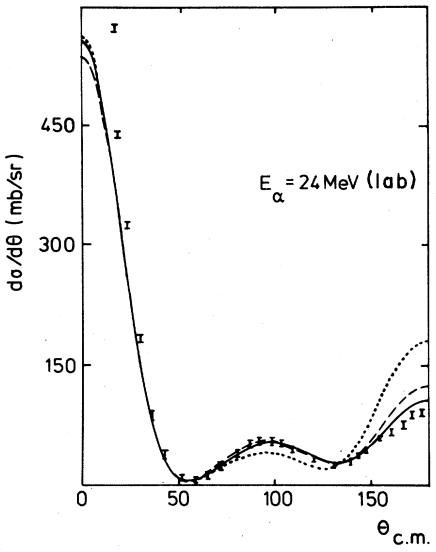


FIG. 6. Elastic differential $d\alpha$ cross sections without Coulomb interaction. Solid line: fish bone optical model. Broken line: result by Charnomordic *et al.* Dotted line: model by Charnomordic *et al.* with $^2S_{1/2}$ wave interaction replaced by our second choice of a phenomenological potential (compare Fig. 3). Experimental data taken from Stewart *et al.* (Ref. 30).

Second, the shape of the direct part of the N-$\alpha$ potential has not been determined by microscopic calculation. The saturation property of the nucleon-nucleon force can phenomenologically be represented by a hard core. The hard core causes short range correlations of the nucleons which lead to a large kinetic energy density. In the effective interaction of clusters, this kinetic energy density has an influence on the shape of the direct potential.[23,31] It decreases the depth at short distances, and for this reason we used a Woods-Saxon shape instead of a Gaussian shape. Third, we did not take into account distortions of the $\alpha$ particle, in our N-$\alpha$ potential, and we did not care too much about N-$\alpha$ phase shifts above 18 MeV. Fourth, we have neglected all three-body forces, as discussed in Sec. III E.

We were not able to study all these effects quantitatively, but we believe that the Coulomb effect is the most important, especially in breakup scattering. Here, the agreement between theory and experiment is rather bad in certain kinematical regions.

It is interesting to compare the present results with results of Faddeev calculations with phenomenological N-$\alpha$ potentials. Knowing the importance of the Pauli principle we may ask: Why do the results of Charnomordic, Fayard, and Lamot (CFL) agree so well with experiment? Let us recall that the main ingredient of the present Faddeev calculation, besides masses and a phenomenological n-p potential, has been a set of N-$\alpha$ wave functions at chosen interpolation energies. If we want to compare models we may as well compare those wave functions. Figure 10 shows the N-$\alpha$ wave function at 10 MeV in the $^2S_{1/2}$ wave. The full line is the resonating group model wave function; the first node arises from orthogonality with respect to one Pauli-forbidden state. The dashed line

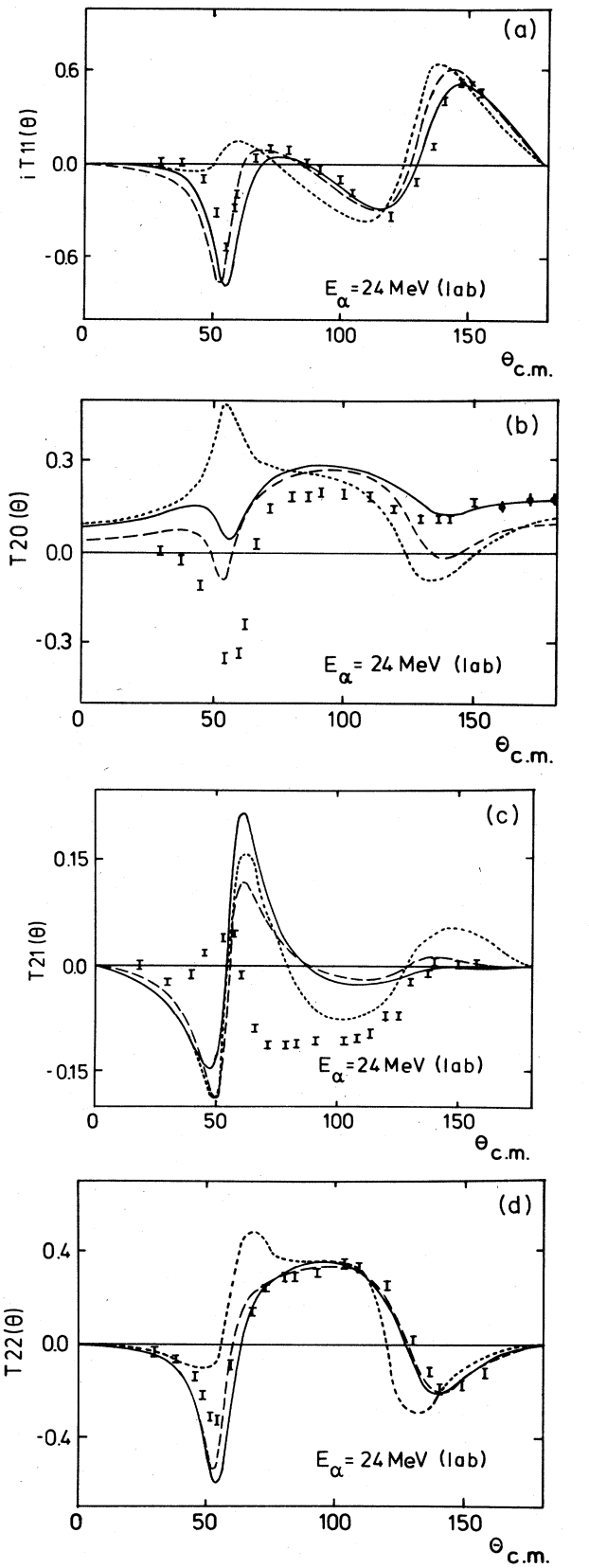


FIG. 7. Analyzing powers of elastic $d\alpha$ scattering. Marking of lines as in Fig. 6. Experimental data are taken from Grüebler *et al.* (Ref. 30).

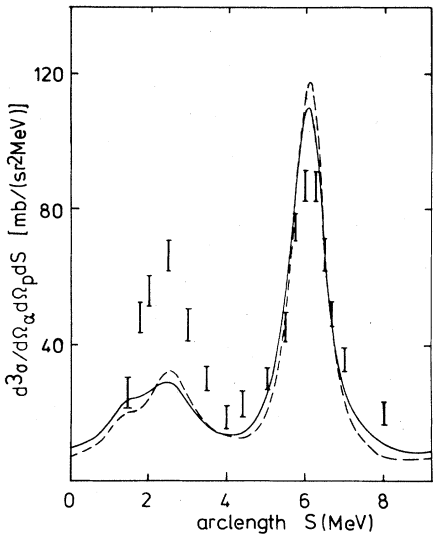


FIG. 8. Breakup cross sections at $E_\alpha = 15$ MeV (lab), $\theta_\alpha = 17.1°$, $\theta_p = 50.5°$, and $\Delta\phi_{\alpha p} = 180°$. The solid line is calculated with the fish bone optical model, the broken line with the potentials of Charnomordic *et al.*, and experimental data are taken from Kôersner *et al.* (Ref. 30).

shows the wave function of the CFL potential. It has a node at a somewhat smaller distance and, in comparison with the resonating group wave function, it underestimates a little the probability of finding the nucleon inside the $\alpha$ particle. But it looks rather similar to the resonating group wave function. Also, in the $^2P_{3/2}$ and $^2P_{1/2}$ partial waves, the resonating group wave functions and the wave functions of the CFL potential look similar; at short distances the wave functions of the CFL potential have somewhat larger values than the resonating group wave functions. In Figs. 6–9 we have plotted Faddeev results obtained with the CFL potential in dashed lines. We

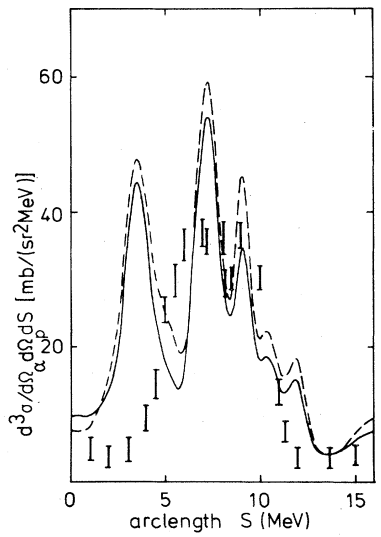


FIG. 9. Breakup cross sections at $E = 15$ MeV (lab), $\theta_\alpha = 17.1°$, $\theta_p = 17.1°$, and $\Delta\phi_{\alpha p} = 180°$. Marking of lines and experimental data as in Fig. 8.

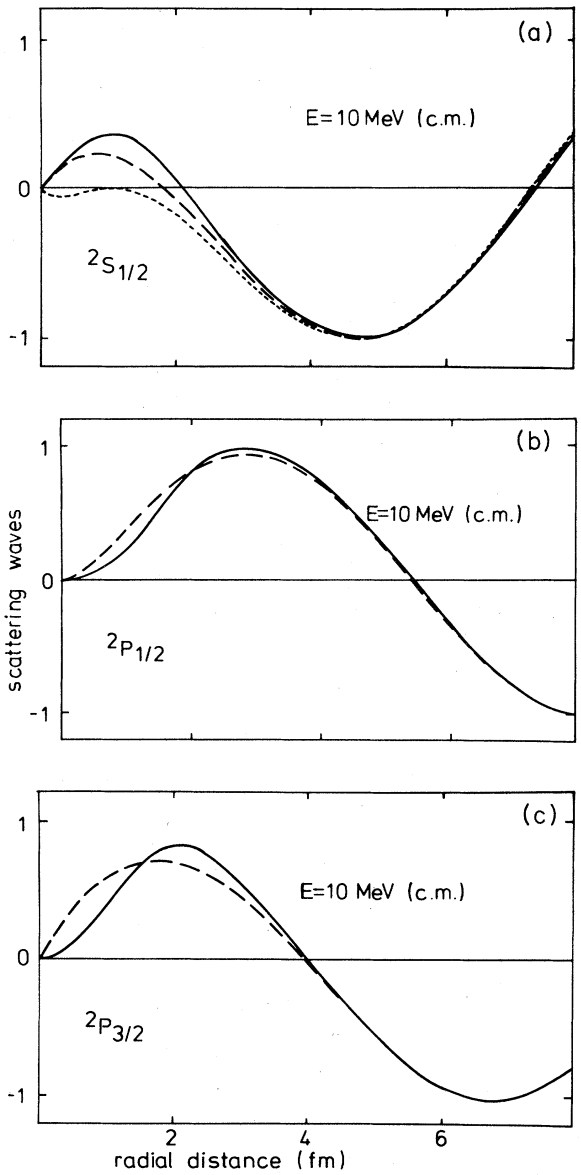


FIG. 10. Comparison of neutron-alpha wave functions calculated with the fish bone optical model (solid lines), with the phenomenological model of Charnomordic *et al.* (broken lines), and with our second choice of a phenomenological potential (dotted line, only $^2S_{1/2}$ wave).

are tempted to say that the Faddeev results of Charnomordic, Fayard, and Lamot agree rather well with experiment because their N-$\alpha$ wave functions do not differ too much from resonating group wave functions.

As a counter example, we took another phenomenological N-$\alpha$ potential in the $^2S_{1/2}$ wave. This second phenomenological potential also reproduces the experimental n-$\alpha$ shifts of the elastic energy region rather well (see the dotted line in Fig. 3). But its wave functions are not similar to resonating group wave functions. The dotted line in Fig. 10 shows the wave function at 10 MeV. Also, this potential has a rising phase shift between 25 and 40 MeV which means that, without any microscopic

foundation, it simulates some $\alpha$-particle distortion effect. In a Faddeev calculation for d-$\alpha$ elastic scattering with $E_\alpha = 24$ MeV (lab) we have used this second phenomenological N-$\alpha$ potential in the $^2S_{1/2}$ partial wave, together with CFL potentials in the $^2P_{3/2}$ and $^2P_{1/2}$ waves. The result is shown by the dotted line in Figs. 6 and 7. Even though the $^2S_{1/2}$ partial wave does not dominate the scattering process, we immediately get worse agreement with experiment at backward angles. This may demonstrate that the off-shell behavior of the effective N-$\alpha$ interaction, as imposed by the Pauli principle, plays an important role, and that it is not sufficient just to reproduce the experimental phase shifts of the elastic energy region.

## V. SUMMARY

The resonating group Faddeev method has been formulated and applied to deuteron-alpha elastic and breakup scattering. The reduction of the six-nucleon problem to an effective three-body problem is done in several steps.

(1) The three-cluster resonating group model for the np$\alpha$ system, without distortion of the $\alpha$ particle, is approximated by the fish bone optical model. In the latter model, the effective interaction is decomposed into three two-body interactions and a three-body interaction.

(2) The fitting parameters of the fish bone optical model are determined by the condition that the two-body potentials reproduce experimental two-body data.

(3) The effective two-body potentials are brought into a separable form of rank $r$ by a unitary interpolation method. In the elastic region, the separable potentials do not only reproduce the phase shift, but also reproduce the wave function of the original potential.

(4) Two-body wave functions of the separable potentials are compared with (off-shell transformed) resonating group wave functions, in order to establish equivalence with the resonating group model.

(5) The three-body potential is dropped.

By solving the Faddeev equations in a test case it is seen that the high-energy phase shift of the two-body potentials has only little influence on the three-body observables, at energies under consideration. The half-shell property of the two-body potentials, in the elastic region, does have an influence on the three-body observables. At backward angles, where the missing Coulomb contributions are expected to be small, the elastic d-$\alpha$ differential cross section and analyzing powers of the resonating group Faddeev model agree better with experiment than those of two phenomenological models; the agreement with experiment is worse in the model which deviates most of the resonating group model.


[1]J. A. Wheeler, Phys. Rev. **52**, 1083 (1937); K. Wildermuth and Th. Kanellopoulos, Nucl. Phys. **7**, 150 (1958); K. Wildermuth and Y. C. Tang, *A Unified Theory of the Nucleus* (Vieweg, Braunschweig, 1977).

[2]Y. C. Tang, M. Le Mere, and D. R. Thompson, Phys. Rep. **47**, 167 (1978).

[3]R. H. Maulbetsch, Ph.D. dissertation, Fakultät für Physik, Universität Tübingen, 1971 (unpublished).

[4]N. E. Fuchs, Ph.D. dissertation, Fakultät für Physik, Universität Tübingen, 1974 (unpublished).

[5]R. Mader, Test von Variationsverfahren bei Aufbruchsreaktionen an einem exakt lösbaren Dreiteilchenproblem (Burg, Basel, 1976).

[6]M. Yahiro, Y. Iseri, M. Kamimura, and M. Nakano, submitted to Phys. Lett. B.

[7]E. W. Schmid and H. Ziegelmann, *The Quantum Mechanical Three-Body Problem* (Vieweg, Braunschweig, 1974).

[8]E. W. Schmid (unpublished).

[9]E. W. Schmid, Phys. Rev. C **21**, 691 (1980).

[10]E. W. Schmid (unpublished).

[11]E. W. Schmid, Z. Phys. A **297**, 105 (1980).

[12]E. W. Schmid, Z. Phys. A **302**, 311 (1981).

[13]R. Kircher and E. W. Schmid, Z. Phys. A **299**, 241 (1981).

[14]E. W. Schmid, S. Saito, and H. Fiedeldey, Z. Phys. A **306**, 37 (1982).

[15]E. W. Schmid, M. Orlowski, and Bao Cheng-guang, Z. Phys. A **308**, 237 (1982).

[16]P. Doleschall, Nucl. Phys. **A201**, 264 (1972).

[17]B. Charnomordic, C. Fayard, and G. H. Lamot, Phys. Rev. C **15**, 864 (1977).

[18]Y. Koike (private communication).

[19]D. A. Zaikin, Nucl. Phys. **A357**, 584 (1971).

[20]G. R. Satchler, L. W. Owen, A. J. Elwyn, G. L. Morgan, and R. L. Walter, Nucl. Phys. **A112**, 1 (1968).

[21]D. J. Ernst, C. M. Shakin, and R. M. Thaler, Phys. Rev. C **8**, 46 (1973).

[22]I. Reichstein and Y. C. Tang, Nucl. Phys. **A158**, 529 (1970).

[23]S. Saito, Y. Akaishi, H. Klar, S. Nakaichi-Maeda, E. W. Schmid, and G. Spitz (unpublished).

[24]E. W. Schmid, Proceedings of the International Symposium on Few Particle Problems in Nuclear Physics, Dubna, 1979, p. 174.

[25]E. W. Schmid, Nucl. Phys. **A416**, 347c (1984).

[26]S. Nakaichi-Maeda and E. W. Schmid, Z. Phys. A **318**, 171 (1984).

[27]S. Nakaichi-Maeda and E. W. Schmid, Z. Phys. A **315**, 287 (1984).

[28]K. Hahn, Ph.D. dissertation, Fakultät für Physik, Universität Tübingen, 1983 (unpublished).

[29]K. Hahn, in *Proceedings of the Tenth International Conference on Few Body Problems in Physics, Karlsruhe, 1983* (North-Holland, Amsterdam, 1984), Vol. II, p. 425.

[30]L. Stewart, J. E. Brolley, Jr., and L. Rosen, Phys. Rev. **128**, 707 (1962); W. Grüebler, R. E. Brown, F. D. Correll, R. A. Hardekopf, N. Jarmie, and G. G. Ohlsen, Nucl. Phys. **A331**, 61 (1979); I. Kôersner, L. Glantz, A. Johansson, B. Sundquist, N. Nakamura, and H. Noya, *ibid.* **A286**, 431 (1977).

[31]G. Spitz, H. Klar, and E. W. Schmid, in *Proceedings of the Tenth International Conference on Few Body Problems in Physics, Karlsruhe, 1983* (North-Holland, Amsterdam, 1984), Vol. II. p. 407.